Oecologia (2023) 201:771–782
https://doi.org/10.1007/s00442-023-05322-z

COMMUNITY ECOLOGY – ORIGINAL RESEARCH

Nutrients strengthen density dependence of per-capita growth and mortality rates in the soil bacterial community

Bram W. Stone[1,2] · Steven J. Blazewicz[3] · Benjamin J. Koch[2,4] · Paul Dijkstra[2,4] · Michaela Hayer[2] · Kirsten S. Hofmockel[1,5] · Xiao Jun Allen Liu[6] · Rebecca L. Mau[2] · Jennifer Pett-Ridge[3,7] · Egbert Schwartz[2,4] · Bruce A. Hungate[2,4]

Received: 19 November 2021 / Accepted: 15 January 2023 / Published online: 27 February 2023

Abstract

Density dependence in an ecological community has been observed in many macro-organismal ecosystems and is hypothesized to maintain biodiversity but is poorly understood in microbial ecosystems. Here, we analyze data from an experiment using quantitative stable isotope probing (qSIP) to estimate per-capita growth and mortality rates of bacterial populations in soils from several ecosystems along an elevation gradient which were subject to nutrient addition of either carbon alone (glucose; C) or carbon with nitrogen (glucose + ammonium-sulfate; C + N). Across all ecosystems, we found that higher population densities, quantified by the abundance of genomes per gram of soil, had lower per-capita growth rates in C + N-amended soils. Similarly, bacterial mortality rates in C + N-amended soils increased at a significantly higher rate with increasing population size than mortality rates in control and C-amended soils. In contrast to the hypothesis that density dependence would promote or maintain diversity, we observed significantly lower bacterial diversity in soils with stronger negative density-dependent growth. Here, density dependence was significantly but weakly responsive to nutrients and was not associated with higher bacterial diversity.

Keywords Density dependence · Bacteria · Soil · Quantitative stable isotope probing (qSIP) · Diversity

Introduction

Negative density dependence is a well-studied phenomenon in the field of plant ecology wherein larger populations experience lower rates of growth or recruitment (Janzen 1970; Johnson et al. 2012). It is either brought about by intraspecific competition, where individual plants compete most strongly with individuals of the same species (Chesson 2000), or by the spread of species-specific pathogens and parasites through a population, the rate of spread enhanced by increasing density (Connell 1971; Klironomos 2002). Both mechanisms create negative density dependence, which is understood to reduce competitive exclusion for large populations in a community and, therefore, promote local diversity (Petermann et al. 2008; Levine and HilleRis-Lambers 2009; Bever et al. 2012; Johnson et al. 2012). Less is known about the existence and causative mechanisms of this phenomenon in soil microbial communities, due to both the difficulty in measuring population vital rates as well as population densities in situ.

Communicated by Kendi Davies.

✉ Bram W. Stone
bram.stone@pnnl.gov

1 Earth and Biological Sciences Directorate, Pacific Northwest National Laboratory, Richland, WA, USA

2 Center for Ecosystem Science and Society, Northern Arizona University, Flagstaff, AZ, USA

3 Physical and Life Sciences Directorate, Lawrence Livermore National Lab, Livermore, CA, USA

4 Department of Biological Sciences, Northern Arizona University, Flagstaff, AZ, USA

5 Department of Agronomy, Iowa State University, Ames, IA, USA

6 Department of Microbiology and Plant Biology, Institute for Environmental Genomics, University of Oklahoma, Norman, OK, USA

7 Life and Environmental Sciences Department, University of California Merced, Merced, CA, USA

Studies of density dependence of microbial populations in microcosms exist in the classical ecological literature (Gause 1934; Allee 1941; Tilman 1977) and more recently as tests of current ecological theory (Jessup et al. 2005; Cadotte et al. 2006; Letten et al. 2018; Rovere and Fox 2019). Both negative and positive density dependence have been observed in populations of cultured bacteria measuring either survival or growth (Phaiboun et al. 2015; Kaul et al. 2016). However, the soil environment differs from many microcosm experiments in that its structure constrains microbial interactions relative to laboratory cultures. In soil, a small portion of habitable surface is colonized by microorganisms who are aggregated and isolated from other colonies inside biofilms (Young et al. 2008; Flemming and Wuertz 2019). This isolation is thought to underpin the microbial diversity observed in soils by avoiding competitive exclusion (Kerr et al. 2002; Carson et al. 2010; Tecon and Or 2017). Further, soil microbial communities are primarily limited by available carbon or co-limited by carbon and nitrogen (Aldén et al. 2001; Demoling et al. 2007). Within soil biofilms and aggregates themselves, close associations with between different species likely confer important synergistic advantages (Nadell et al. 2016). However, the number of different species within the local vicinity of any given bacterium (< 20 µm) is likely to be low (Raynaud and Nunan 2014) while binary fission has been observed in many instances to intensify clonal aggregation within the biofilm (Nadell et al. 2016), making conspecific interactions quite likely. Thus, in soil, the relative strength of conspecific competition merits resolution. Conspecific negative density dependence, where larger populations experience lower growth rates, may suggest that competition for nutrients between conspecifics is an important mechanism even within the diverse and interactive soil community.

A relatively new technique, quantitative stable isotope probing (qSIP) with $^{18}O–H_2O$ overcomes the problem of measuring microbial populations in situ by estimating rates of DNA synthesis by quantifying the rate of ^{18}O incorporation into nucleic acids from water, and then using a mathematical model to estimate growth and mortality rates. qSIP can be applied to natural microbiomes to estimate these vital rates for each individual taxon in the bacterial assemblage. However, the rates estimated through qSIP represent an average of many cells from a small volume of soil without accompanying spatial information. Thus, while we use the term "population" to describe the collective growth and mortality of a single bacterial taxon, it represents an aggregate measure of sub-populations with varying sizes and degrees of spatial isolation.

Past observations using qSIP to assess density dependence showed differing patterns. An Arizona grassland showed density-dependent mortality, but not growth, measured over a 10-day period (Koch et al. 2018). In contrast, a California grassland showed density *independent* mortality during the first 3 h after an early-season wet-up event, whereas growth was density dependent during this time period (Blazewicz et al. 2020). However, because competition for nutrients is an important dynamic in soil systems, it may be valuable to explore microbial response to nutrients in order to understand the degree of competition and density dependence among soil microorganisms. Higher nutrient availability may either alleviate or intensify competition between conspecifics over a set time period which is likely to be influenced by population density.

We hypothesized that larger populations would have lower per-capita growth rates due to intraspecific competition than smaller populations (i.e., growth rates will be lower as population density increases). Further, nutrient addition was hypothesized to alleviate intraspecific competition given the short experimental duration (Steen and Scrosati 2004; Cabaço et al. 2013), although the opposite patterns have been observed (Morris 2003; Wang et al. 2015). Regardless of the specific mechanism, negative density dependence should promote diversity (Johnson et al. 2012) as larger, more slowly growing bacterial populations are unable to outcompete and exclude smaller, faster growing populations. Thus, bacterial diversity was hypothesized to be higher in soils where negative density dependence is stronger. This hypothesis is predicated on competition for limiting resources which is a widespread ecological phenomenon and present in microbial communities (Hibbing et al. 2010). The absence of any relationship between diversity and density dependence may indicate that other mechanisms are more important determinants of bacterial diversity in soils.

To summarize, the main hypotheses were:

H1. Larger bacterial populations will have lower per-capita growth rates
H2. The strength of the density dependence relationship will be lower in nutrient-amended soils
H3. Soils with stronger negative density dependence will have higher bacterial diversity

To test these hypotheses, per-capita growth and mortality rates for individual bacterial populations were quantified using qSIP with $^{18}O–H_2O$ in soils under ambient and elevated nutrient profiles.

Methods

Sample collection and isotope incubation

Data were analyzed from samples collected, manipulated, and published previously (Liu et al. 2017, 2020; Morrissey et al. 2017, 2019; Li et al. 2019). Reiterated here, three

replicate soil samples were collected from the top 10 cm of plant-free, open meadow patches in four ecosystems along the C. Hart Merriam elevation gradient in Northern Arizona. From low to high elevation, these sites were located in the following environments: desert grassland (GL; 1760 m, 35.58° N, 111.57° W), piñon pine–juniper woodland (PJ; 2020 m, 35.50° N, 111.62° W), ponderosa pine forest (PP; 2344 m, 35.42° N, 111.67° W), and mixed conifer forest (MC; 2620 m, 35.35° N, 111.73° W). Sites in order of elevation (GL, PJ, PP, MC) were characterized by decreasing mean annual temperatures (MAT): 8.5 °C, 7 °C, 5.5 °C, 4 °C and increasing mean annual precipitation (MAP): 230 mm, 380 mm, 660 mm, 760 mm (Morrissey et al. 2019). In contrast, soil pH did not vary in a distinct gradient along elevation: 6.9, 6.2, 5.8, and 6.3 (GL, PJ, PP, and MC) (Liu et al. 2017). Soils were air-dried for 24 h at room temperature (~ 23 °C), homogenized, and passed through a 2 mm sieve before being stored at 4 °C for another 24 h. Three treatments were provided to these soils through the addition of water at 70% water-holding capacity: water alone (control), with glucose (C treatment; 1000 µg C g^{-1} dry soil), or with glucose and a nitrogen source (C + N treatment; $[NH_4]_2SO_4$ at 100 µg N g^{-1} dry soil). Amendment concentrations were matched to parallel samples amended with ^{13}C–glucose (data not reported here). Glucose additions were chosen to facilitate detection of ^{13}C label in microbial DNA. Nitrogen was added in a 10:1 ratio, matching the soil C:N ratios of the characterized sites (Liu et al. 2017). This design resulted in three soil samples per ecosystem per treatment (across four ecosystems and three treatments, $n = 36$). To track growth through isotope assimilation, all experimental replicates ($n = 36$) were provided ^{18}O–enriched water in all treatments (97 atom %) with a matching set of control samples that was provided water at natural-abundance ^{18}O ($n = 36$). All soils samples ($n = 72$) were incubated in the dark for 1 week at room temperature (~ 23 °C). Following incubation, soils were frozen at − 80 °C for 1 week prior to DNA extraction.

Quantitative stable isotope probing

The following procedure is reiterated here as conducted previously (Morrissey et al. 2017, 2019; Li et al. 2019). DNA extraction was performed on 0.5 g of ^{18}O-incubated soils and corresponding controls. To quantify the degree of ^{18}O isotope incorporation into bacterial DNA, the qSIP protocol (Hungate et al. 2015) was used, though modified slightly as reported previously (Morrissey et al. 2017, 2019; Li et al. 2019). Microbial growth was quantified based on DNA buoyant density through the method of density fractionation by adding 1 µg of DNA to 2.6 mL of saturated CsCl solution in combination with a gradient buffer (200 mM Tris, 200 mM KCL, 2 mM EDTA) in a 3.3 mL OptiSeal ultracentrifuge tube (Beckman Coulter, Fullerton, CA, USA). The solution was centrifuged to produce a gradient of increasingly labeled (heavier) DNA in an Optima Max bench top ultracentrifuge (Beckman Coulter, Brea, CA, USA) with a Beckman TLN-100 rotor (127,000 × g for 72 h) at 18 °C. Each post-incubation sample was thus converted from a continuous gradient into approximately 20 fractions (150 µL) using a modified fraction recovery system (Beckman Coulter). The density of each fraction was measured with a Reichart AR200 digital refractometer (Reichert Analytical Instruments, Depew, NY, USA). Following purification from CsCl buffer, DNA as measured using the Quant-IT PicoGreen dsDNA assay (Invitrogen) and a BioTek Synergy HT plate reader (BioTek Instruments Inc., Winooski, VT, USA). Fractions between densities of 1.640 and 1.735 g cm^{-3} were retained, representing DNA-containing fractions, producing on average 15–16 fractions per sample in all treatments. Bacterial 16S rRNA gene copies were quantified using qPCR using primers excluding non-bacterial sequences (*Eub* 515F: AAT GAT ACG GCG ACC ACC GAG TGC CAG CMG CCG CGG TAA, 806R: CAA GCA GAA GAC GGC ATA CGA GGA CTA CVS GGG TAT CTA AT). Following qPCR quantification, all retained sample-fractions were sequenced for the 16S V4 region (515F: GTG YCA GCM GCC GCG GTA A, 806R: GGA CTA CNV GGG TWT CTA AT) on an Illumina MiSeq (Illumina, Inc., San Diego, CA, USA). In addition to the ^{18}O-incubated qSIP soils, DNA from the same soil samples were extracted prior to incubation and subject to qPCR and Illumina sequencing as above, but without fractionation, in order to assess initial bacterial population size and identities.

Sequence processing and qSIP analysis

Sequence data and sample metadata have been previously deposited in NCBI Sequence Read Archive under the project number PRJNA521534. Independently from previous publications, we processed raw sequence data of forward and reverse reads (FASTQ) within the QIIME 2 environment (release 2018.6) (Bolyen et al. 2019) and denoised sequences with the DADA2 pipeline (Callahan et al. 2016); in both cases following standard settings outlined in QIIME 2. We resolved the remaining sequences into amplicon sequence variants (ASVs, at 100% sequence identity) against the SILVA 132 database (Quast et al. 2013) using an open-reference Naïve Bayes feature classifier implemented within QIIME2 by scikit-learn (Pedregosa et al. 2011). We removed samples with less than 3,000 sequence reads, non-bacterial lineages (Archaea: 6.9% of sequence reads; Eukarya: < 0.001%; mitochondria: 0.1%; chloroplast: 0.1%), and global singletons and doubletons. For the correct quantification of bacterial 16S rRNA gene copies within each fraction given our use of bacterial-specific qPCR primers, removal of Archaeal lineages was necessary. This produced

a dataset of 99,465 bacterial ASVs and 34,886,320 sequence reads. For each ASV, we converted the normalized sequence read abundances in each fraction to the number of 16S rRNA gene copies per gram dry soil based on the known amount of dry soil equivalent added to the initial extraction. This allows us to express absolute population densities, rather than relative abundances. To ensure that estimates of growth and mortality did not include infrequent taxa, whose enrichment is difficult to accurately quantify, we removed ASVs that failed to appear in two of the three replicates of a site-treatment combination ($n = 3$) and at least five of the fractions within each of those two replicates. This allowed any ASVs filtered out of one treatment to appear in another if they met the frequency threshold. In total, 2,277 bacterial ASVs met these thresholds for which we proceeded to calculate growth and mortality rates. These taxa represent only 2.3% of the total number of ASVs sequenced but correspond to 55.8% of all sequence reads.

For each bacterial taxon (i) in a given replicate, we calculated the molecular weight of DNA in samples amended with natural-abundance ^{18}O–water ($M_{16O,i}$) and in the samples amended with 97 atom % ^{18}O–water ($M_{18O,i}$) using the formulae from Hungate et al. (2015):

$$M_{16O,i} = 0.496\left(\frac{W_{16O,i} - 1.646057}{0.083506}\right) + 307.691 \quad (1)$$

$$M_{18o,i} = \left(\frac{W_{18o,i} - W_{16o,i}}{W_{16o,i}}\right) \cdot M_{16o,i} \quad (2)$$

where $W_{16O,i}$ indicates the weighted average buoyant density of taxon i in replicates amended with water at natural-abundance ^{18}O (i.e., unlabeled replicates) and $W_{18O,i}$ indicates the weighted average buoyant density of taxon i in replicates amended with water at 97 atom % ^{18}O–water (i.e., labeled replicates). Weighted density values were calculated as the sum of taxon i's proportional abundance across all density-separated fractions multiplied by the corresponding density (g ml^{-1}) of the fraction. As the density of unlabeled DNA for each taxon should be the same across all unlabeled replicates, $W_{16O,i}$ here represents the average value of taxon i's unlabeled density while $W_{18O,i}$ represents the per-replicate value of taxon i's labeled density.

We then calculated per-capita growth and mortality rates of each remaining bacterial ASV in a distinct labeled replicate following the approach of Koch et al. (2018). Growth rates (b) for each bacterial taxon in each replicate were calculated by

$$b_i = 1\mathrm{n}\left(\frac{N_{i,t}}{N_{16o,i,t}}\right) \cdot \frac{1}{t} = 1\mathrm{n}\left(\frac{N_{i,t}}{N_{i,t} \cdot [(M_{Heavy,i} - M_{18o,i})/(M_{Heavy,i} - M_{16o,i})]}\right) \cdot \frac{1}{t} \quad (3)$$

where $N_{i,t}$ indicates the total number of bacterial 16S copies attributed to taxon i after the incubation (i.e., at time t) and $N_{16O,i,t}$ indicates the number of unlabeled 16S copies of taxon i at time t (i.e., whose oxygen atoms contain no ^{18}O labeling) which is estimated by multiplying the total number of 16S copies of taxon i by the proportion of unlabeled 16S copies. Here, $M_{heavy,i}$ indicates the molecular weight of ^{18}O-labeled DNA labeled at 60%, the theoretical maximum (assuming the percentage of oxygen derived from ^{18}O–water in a new DNA molecule per Koch et al. (2018)) equal to the sum of $M_{16O,i}$ and the constant 7.246482.

Assuming exponential growth, mortality rates (d) were calculated as the log-ratio of initial (and unlabeled) 16S copies to remaining unlabeled 16S copies for each taxon i:

$$d_i = 1\mathrm{n}\left(\frac{N_{16O,i,t}}{N_{16o,i,0}}\right) \cdot \frac{1}{t} \quad (4)$$

where $N_{16O,i,0}$ indicates the unlabeled 16S gene abundance of taxon i at time 0 (measured by qPCR). In other words, mortality rates indicate the turnover of the initial population and should, therefore, be a negative number. To make reporting more intuitive, we multiplied mortality rates by − 1 to make them positive.

Correcting 16S gene copy number variance

To account for variation in 16S rRNA gene copy numbers across prokaryote taxa, which may affect community-wide density dependence patterns, we converted all 16S gene abundances to genome abundances (g soil^{-1}) based on the estimated number of 16S gene copies per genome. We roughly followed the approach of Louca et al. (2018). We downloaded the Ribosomal rRNA database (rrnDB, version 5.7, last modified January 8, 2021) (Stoddard et al. 2015). To improve the quality of any matching, we cross-referenced all accession numbers in the rrnDB with those from the list of NCBI RefSeq annotated genomes marked as "complete genomes" (ftp://ftp.ncbi.nlm.nih.gov/genomes/GENOME_REPORTS/prokaryotes.txt, downloaded February 25, 2022). In addition, we removed any 16S sequences in rrnDB greater than 2,000 bp. This produced 16S rRNA gene copy estimates for 20,048 complete genomes. Since many organisms have multiple listed genome accessions, we aligned the representative sequences of our 2,277 qSIP-resolved ASVs against the longest 16S sequences from each unique prokaryote taxon in the rrnDB (8518 distinct taxa) using the AlignSeqs function in the DECIPHER package in

R (Wright 2016). Following alignment, we then calculated phylogenetic distances using the Jukes–Cantor base substitution model (Jukes and Cantor 1969). Lastly, we identified the phylogenetic distance between each qSIP ASV and the nearest complete genome (i.e., the nearest sequenced taxon distance or NSTD). Louca et al. estimated that NSTD values greater than 0.15 produced inaccurate 16S gene copy number estimates (2018). Following this cut-off, we were able to produce accurate 16S gene copy number estimates for 1426 (62.6%) of our bacterial ASVs (supplemental Fig. 1). For taxa beyond this threshold (i.e., for which an estimate was inaccurate), we applied the median 16S rRNA gene copy number of 2 per genome.

Statistical analysis

We tested whether initial population density (genomes g $soil^{-1}$) and nutrient amendment significantly affected per-capita population rates, using two linear hierarchical mixed models in the lme4 R package, one for per-capita growth rates and another for per-capita mortality rates. In order to capture potential changes to per-taxon density-dependent slopes across treatments, analyses were limited to 524 bacterial ASVs that occurred in every treatment and at least three times per treatment. This group represented 37.0% of all bacterial sequence reads. We also examined whether a universal density dependence relationship, compared to models allowing for taxon-specific density-dependent relationships produced a more parsimonious fit. By comparing hierarchical models with and without taxon-specific slopes in the random terms, we identified whether taxon-specific density dependence was important to growth and mortality rates.

With per-capita growth and mortality rates as the response variable, we selected for optimal random components by adding individual terms and comparing models using AIC scores. With respect to taxon-specific vs. universal density dependence, the optimal random model structure did not feature independent slopes for taxonomic identity (i.e., no taxon-specific density dependence relationships) (supplemental Table 1). Using individual linear models, we further confirmed that there was no trend in per-taxon density-dependent slopes across population sizes (supplemental Fig. 2). Similarly, phylum-specific density dependence was not a feature of the optimal random model structure (supplemental Table 1), and we did not observe any significant trend in density dependence relationships across taxa from different phyla (supplemental Fig. 3). We used the model structure with the lowest combined AIC score across both growth and mortality rates. We thus applied the following model structure:

$$per\ capita\ rate \sim \log_{10}(pop_0) * trt + (1|phylum/tax\ ID/site) \quad (5)$$

Here and hereafter, the first two explanatory terms separated by asterisks represent interacting fixed effects (pop_0 = initial population expressed as genomes per g dry soil, trt = nutrient treatment) while all others separated by addition terms indicate random model effects. We tested the effect of growth and mortality-related processes during the incubation period on final population densities (pop_7) using hierarchical models with identical random terms as in Eq. 5:

$$\log_{10}(pop_7) \sim per\ capita\ rate * trt + (1|phylum/tax\ ID) + (1|site) \quad (6)$$

For the models expressed in Eqs. 5 and 6, we obtained *p* values for fixed effects terms from the lmerTest *R* package using the Satterthwaite method to approximate the necessary degrees of freedom for each comparison and we obtained the marginal coefficient of determination (R_m^2) values for fixed effects terms as well as the conditional coefficient of determination (R_c^2) values for both fixed and random terms using the modified Nakagawa method (2017) as implemented in the MuMIn R package.

Lastly, to test H3, we constructed linear hierarchical models specifying sample-specific density-dependent growth and mortality as random terms and extracting the corresponding slope coefficients ($n = 36$):

$$per\ capita\ rate \sim \log_{10}(pop_0) * trt + (\log_{10}(pop_0)\,|\,sample) \quad (7)$$

We then compared these estimates of the density-dependent growth and mortality to both the ASV richness and Simpson evenness of each sample post-incubation, using the 2277 ASVs for which a growth and mortality rate could be calculated (thus limiting the influence of dormant or inactive organisms, or extracellular DNA on diversity estimates). We used linear models to determine whether there was a significant relationship between density-dependent processes and community diversity.

Results

The relative proportions of major bacterial phyla were consistent across multiple methods of enumeration, as well as the multiple subsets of the community utilized for statistical analyses (supplemental table 3). Across all 99,465 bacterial ASVs, the largest representative phyla were either the Actinobacteria (mean ± 1 SE: 33.7 ± 1.5%) or the Proteobacteria (25.8 ± 2.1%) which together accounted for the majority of sequence reads (Fig. 1A) in every soil replicate. Among the 2,277 bacterial ASVs for which growth and mortality rates could be resolved, the Actinobacteria

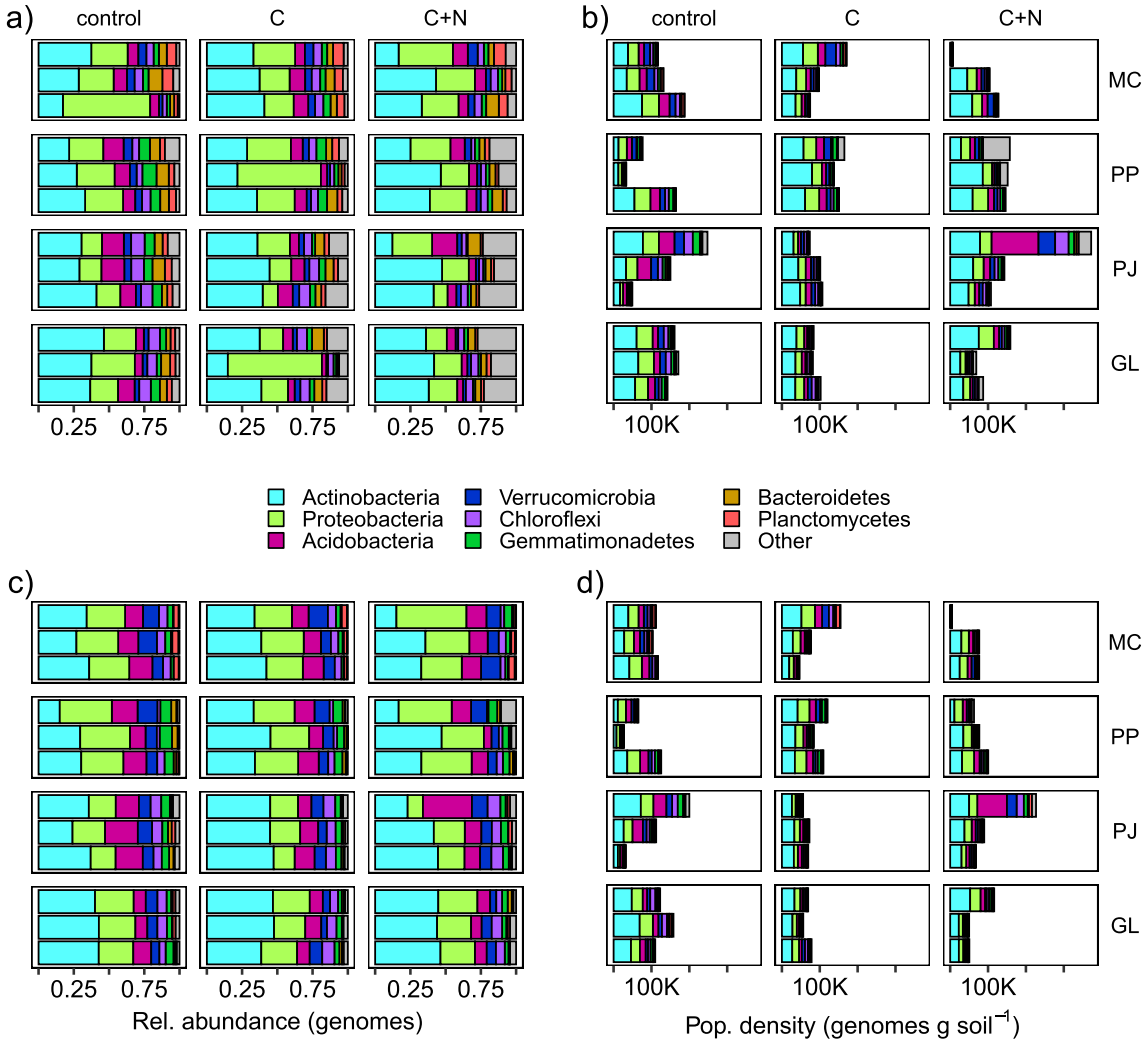

Fig. 1 Composition and abundance of major bacterial lineages. Bars represent the relative or absolute abundance of bacterial phyla from four ecosystems along an elevational gradient in northern AZ: low-elevation grassland (GL), Piñon pine–juniper forest (PJ), Ponderosa pine forest (PP), and high-elevation mixed conifer forest (MC) and subject to three treatments: water-only (control), glucose-amended (C), and glucose and ammonium-sulfate amended (C + N). Individual bars represent distinct soil replicates collected from each ecosystem and subject to each treatment combination ($n = 3$). **a** Relative (Rel.) abundance of 99,465 bacterial ASVs, grouped by phyla, based on the normalized number of 16S amplicon sequence reads (34,886,320). **b** Population (Pop.) density of 524 bacterial ASVs utilized in statistical analyses based on the number of 16S rRNA gene copies per gram of soil. **c** Rel. abundance of 524 bacterial ASVs utilized in statistical analyses based on the normalized number of genomes per gram of soil. **d** Pop. density of 524 bacterial ASVs utilized in statistical analyses based on the number of genomes per gram of soil

(36.8 ± 1.5%) and Proteobacteria (20.7 ± 0.8%) again accounted for the majority proportion of 16S gene copies per gram soil (Fig. 1B). These same phyla were the most abundant after correcting for per-genome 16S rRNA copy numbers, among the frequently occurring 524 ASVs used in statistical analyses. Actinobacteria (36.6% ± 1.6) and Proteobacteria (26.8 ± 1.2%) represented the majority proportion of bacterial genomes (Fig. 1C, D). The third most abundant lineage was the Acidobacteria, accounting for 8.5 ± 0.6% of all sequence reads but representing a higher proportion of the community subjected to statistical analyses (16S gene abundance: 13.0 ± 0.9%, genomes: 13.2 ± 0.8%) (Fig. 1).

Inconsistent with our first and second hypotheses (H1, H2), bacterial growth rates were only negatively affected by initial population densities in soils amended with carbon and nitrogen ($F_{2, 5520} = 30.9$, $p < 0.001$) (Fig. 2A) (Table 1). Population density did not have a significant negative effect on per-capita growth rates in control soils ($t = -1.4$, df = 4192, $p = 0.17$) or in soils amended with labile carbon alone ($t = -1.3$, df = 5497, $p = 0.19$). Instead, only soils amended with labile carbon and nitrogen had a significant decrease in per-capita growth rates with initial population density ($t = -7.4$, df = 5521, $p < 0.001$) (Fig. 2A). This was counter to our hypothesis that unamended soils would experience

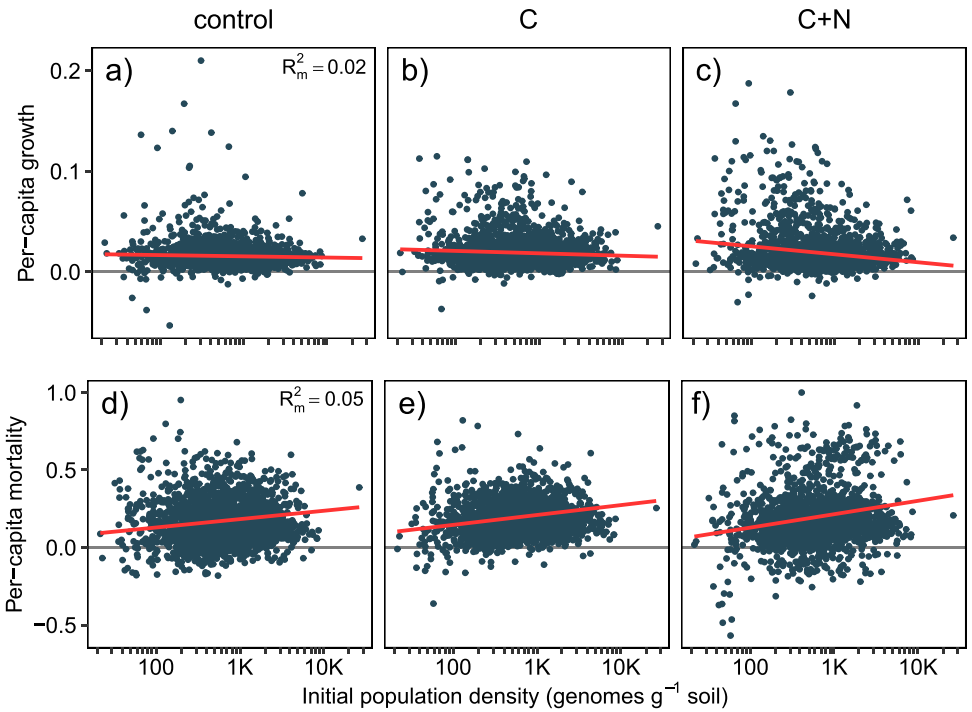

Fig. 2 Relationship between initial population densities and per-capita growth and mortality rates in each treatment measured with ^{18}O–water qSIP. Single points represent per-capita population rates (day^{-1}) plotted against the density of each bacterial population (on a $\log_{10}$ scale), prior to stable isotope incubation, and from each individual soil sample per treatment and replicate collected from four ecosystems along an elevational transect in AZ. Soil treatments are water-only (control), glucose-amended (C), and glucose and ammonium-sulfate amended (C + N). **a** per-capita growth rates. **b** per-capita mortality rates. Lines represent the relationship between per-capita rates and population density in each treatment calculated from hierarchical linear models. R_m^2 values represents the proportional variance in either growth or mortality rates, across all treatments, that is explained by population density in linear hierarchical models

Table 1 Statistical significance of initial population size, soil treatment, and their interaction on per-taxon bacterial growth and mortality rates over a 7-day incubation

	Initial population		Treatment		Population:treatment	
Rate	*F*	*P*	*F*	*P*	*F*	*P*
Growth	27.8	< 0.001	39.1	< 0.001	30.9	< 0.001
Mortality	124.0	< 0.001	4.7	0.009	7.7	< 0.001

Values represent fixed effects coefficients in hierarchical mixed models which were applied across 524 distinct bacterial taxa. Initial population sizes of bacterial ASVs are quantified in terms of genomes g^{-1} dry soil. Soil treatments are water-only (control), glucose-amended (C), and glucose and ammonium-sulfate amended (C + N)

more prominent density-dependent effects (H2). Variance explained by model fixed terms (initial population density and nutrient amendment) was slight and much lower than variance explained when random effects were also included ($R_m^2 = 0.02$, $R_c^2 = 0.44$).

Larger bacterial populations had higher *per-capita* mortality rates during the incubation period in all treatments, and this relationship was also contingent on nutrient amendment (Fig. 2B). Bacterial mortality rates were positively associated with initial population densities—an indication of density dependence—in all soils ($F_{1,\ 1733} = 123.9$, $p < 0.001$) (Table 1). In parallel with trends in growth rates (and in contrast to H2), the slope of the density dependence relationship was significantly steeper in soils amended with carbon and nitrogen ($F_{2,\ 5549} = 7.7$, $p < 0.001$) (Fig. 2B). Also following with growth rates, model fixed terms explained only a small amount of variation in per-capita mortality rates ($R_m^2 = 0.05$, $R_c^2 = 0.34$).

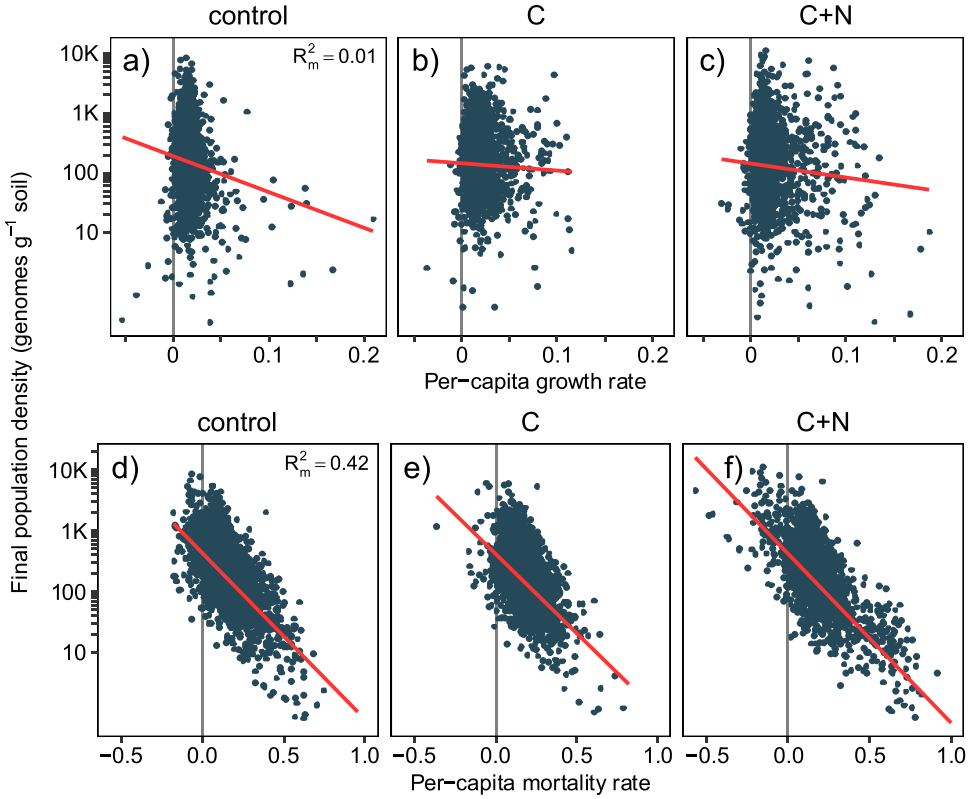

Fig. 3 Relationship between per-capita population rates and final bacterial abundances. Single points represent the density of each bacterial population (on a $\log_{10}$ scale), after stable isotope incubation, plotted against per-capita population rates (day^{-1}), and from each individual soil sample per treatment and replicate collected from four ecosystems along an elevational transect in AZ. Soil treatments are water-only (control), glucose-amended (C), and glucose and ammonium-sulfate amended (C + N). a) Final population density against per-capita growth rates. b) Final population density against per-capita mortality rates. Lines represent the relationship between per-capita rates and final population density in each treatment calculated from hierarchical linear models. R_m^2 values represents the proportional variance in final population density, across all treatments, that is explained by initial population density in linear hierarchical models

While both growth and mortality rates estimated through qSIP are based in part on ^{18}O enrichment and initial population abundances—and would be expected to both be closely related to final population abundances—we observed that only mortality rates were strong predictors of final population densities (Fig. 3). Per-capita growth rates had a significant effect on final population densities ($F_{1, 6281} = 68.1$, $p < 0.001$) but the model explained a small proportion of overall variance ($R_m^2 = 0.01$, $R_c^2 = 0.60$). Further, the relationship between per-capita growth rates and final population densities was inconsistent across treatments ($F_{2, 5755} = 16.6$, $p < 0.001$). Conversely, mortality rates were a significant and strong predictor of final population densities across all treatments ($F_{1, 5624} = 22{,}205.7$, $p < 0.001$, $R_m^2 = 0.42$, $R_c^2 = 0.93$).

Bacterial diversity (among the ASVs for which growth and mortality rates could be calculated) was positively associated with stronger density dependence of growth rates. However, soils with stronger negative density dependence had fewer bacterial ASVs, contrary to our hypothesis for the incubation period (H3). Soils with stronger density dependence of bacterial growth rates (indicated by steeper, more negative slopes) had fewer bacterial ASVs ($F_{1, 33} = 10.3$, $p = 0.003$) (Fig. 4A) and lower evenness among bacterial ASVs (Simpson's evenness: $F_{1, 33} = 4.1$, $p = 0.05$) (Fig. 4C). This pattern was not statistically significant when comparing density dependence of mortality with richness ($F_{1, 34} = 0.52$, $p = 0.47$) or Simpson's evenness ($F_{1, 34} = 2.41$, $p = 0.13$) (Fig. 4D).

Discussion

In the soils studied, bacterial populations across all major phyla showed negative conspecific density dependence (H1, Fig. 2). However, density-dependent signals were generally weak, especially in contrast to the strength of site-specific and taxon-specific signals captured in the random terms of these models and in more detailed hierarchical modeling

(Morrissey et al. 2016, 2019). This suggests that evolutionary history and edaphic properties are stronger drivers of the growth and turnover response of bacterial lineages in these soils than density-dependent processes. In this experiment, and two similar studies, mortality rates were higher than growth rates for almost all taxa (Koch et al. 2018; Blazewicz et al. 2020), and in all cases, soils were dried prior the incubation which was initiated by adding water. Blazewicz et al. note that high, density independent mortality occurred quickly after soil rewetting which was likely caused by either osmotic shock to bacterial cells upon wet-up or the rapid degradation of extracellular DNA that accumulated as the soil dried prior to incubation (2020). Population densities of bacterial ASVs at the end of the incubation corresponded closely to per-capita mortality rates, but not growth rates, indicating the intense control that mortality and turnover processes have on dry-down wet-up design stable isotope incubations. Although density dependence signals were weak across the 7-day incubation, it is possible that over longer time periods, density-dependent dynamics hold a larger influence on bacterial population dynamics in soil.

The design of this study did not exclude any specific density-dependent mechanism from acting on the bacterial community. Intraspecific competition for limited resources is one explanation for this phenomenon and is a fundamental assumption of density-dependent population dynamics, as expressed through habitat carrying capacity studied in a homogenous and aqueous environment (Gause 1934). Phages are also understood to impose negative density dependence on their hosts ("kill the winner"), thus preventing any particular taxa from achieving dominance (Maslov and Sneppen 2017). However, this mechanism has not been demonstrated in a terrestrial setting. In soils and sediments, phage density has been shown to be high, though our understanding of their effect in these environments is nascent (Ashelford et al. 2003; Williamson et al. 2017; Trubl et al. 2018). Phages are almost certainly active in soils, capable of altering soil community structure and function (Braga et al. 2020) and influencing biogeochemical cycling (Kuzyakov and Mason-Jones 2018). In terrestrial environments, phages may only move when pore spaces are saturated, or inside host cells as prophages, and must access bacteria within biofilms (Kuzyakov and Mason-Jones 2018; Vidakovic et al. 2018). Here, the addition of water to soils at the beginning of the experiment may have allowed phages to proliferate and access host cells, causing negative density dependence. A more detailed tracking of viral dynamics in soils is critical to building a thorough understanding of population dynamics and predicting bacterial response to changing conditions such as wet-up and nutrient addition.

In addition to the significance of negative density dependence across the soils studied, there was an interaction between nutrient addition and population rates (H2, Fig. 2). However, there was no evidence that higher nutrient availability alleviated this phenomenon. Instead, the strongest patterns of density dependence were observed where labile nutrients were added (Fig. 2). The addition of limiting nutrients has been shown to intensify competition in plant communities (Campbell and Grime 1992). Given the spatial separation of bacterial populations in soil (Young et al. 2008), it is possible that this conspecific competition was important in the present study. Nutrient amendments may have initially alleviated density dependence patterns in these soils, but ultimately promoted more growth and thus greater negative feedbacks, as higher bacterial densities led to stronger intraspecific competition. Alternatively, phage populations may have been encouraged to switch from lysogenic to lytic stages due to the favorable conditions and higher bacterial growth in nutrient-amended soils (Erez et al. 2017; Howard-Varona et al. 2017).

In addition to conspecific competition and phage predation, changing conditions brought on by the nutrient amendment may have produced the apparent patterns in bacterial density-dependent growth. The use of labile glucose encourages growth across fewer bacterial taxa than amino acids (Dang et al. 2021). Considering growth rates observed in the glucose and nitrogen treatment in this experiment, amendments seem to have selected for fast-growing organisms that were capable of utilizing the majority of added carbon (Stone et al. 2021). The design of the current experiment cannot necessarily disentangle this effect (changes to interspecific competition due to changing conditions) from conspecific competition or from phage predation. Resolution may come from efforts to map interactions in situations with reduced soil connectivity such as drying, e.g., de Vries et al. (2018) or by increasing certain types of interactions such as enrichment of soil phage populations, e.g., Albright et al. (2022).

In the present experiment, bacterial diversity was lower in soils that had stronger negative density dependence contrasting H3 (Fig. 4). Assuming negative density dependence promotes diversity by preventing competitive exclusion, then a longer experimental duration may produce some effect. However, given the spatial structure of soil bacterial communities, it is possible that conspecific density dependence plays very little role in preserving soil bacterial diversity even at longer time scales. Previous studies identified soil edaphic properties and resource stoichiometry as the strongest controls on bacterial diversity (Fierer and Jackson 2006; Delgado-Baquerizo et al. 2017). Larger and more inclusive sequencing data (i.e., containing a combination of prokaryote, eukaryote, or viral) will be important to resolving the specificity and intensity of microbial interactions in soil. Such efforts will help clarify the effects and interactions of competition,

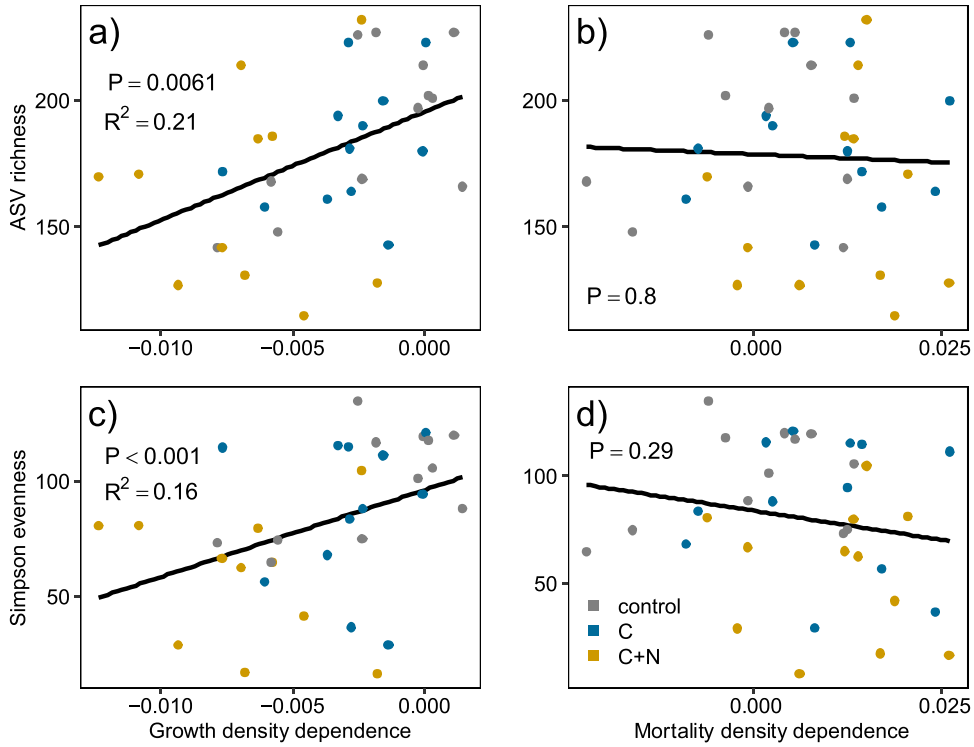

Fig. 4 Relationship between strength of density dependence and bacterial alpha diversity. Single points represent bacterial alpha diversity in replicates from four ecosystems (low-elevation grassland, Piñon pine–juniper forest, Ponderosa pine forest, and high-elevation mixed conifer forest; $n = 3$ of each) plotted against the slopes of the density dependence of per-capita growth and mortality rates. Density dependence slopes represent the change in growth or mortality rate per change in population density ($\log_{10}$-transformed), calculated across the bacterial community. Soil treatments are water-only (control), glucose-amended (C), and glucose and ammonium-sulfate amended (C + N). Top: richness of bacterial amplicon sequence variants (ASVs) compared to the slope of **a** density-dependent growth rates and **b** density-dependent mortality rates. Bottom: evenness of bacterial ASVs ($\log_{10}$ scale) compared to the slope of **c** density-dependent growth rates and d) density-dependent mortality rates

predation, and soil conditions as controls on the diversity of the soil microbiota.

Supplementary Information The online version contains supplementary material available at https://doi.org/10.1007/s00442-023-05322-z.

Acknowledgements We thank the editorial team and two anonymous reviewers for their suggestions and improvements.

Author contribution statement PD, MH, KSH, XJL, RLM, JPR, ES, and BAH designed the experiment and interpreted the findings. XJL, MH, and RLM collected and processed the samples. MH and RLM performed the laboratory work and generated the data. BWS analyzed the data and wrote first draft of manuscript. SJB and BJK interpreted the findings and contributed to the figure design and captions. All the authors contributed meaningfully to revisions.

Funding BWS is grateful for support from the Linus Pauling Postdoctoral Distinguished Fellowship program through Pacific Northwest National Laboratory. This research was supported by grants from the United States Department of Energy's Biological Systems Science Division Program in Genomic Science (Nos. DE-SC0016207 and DE-SCSC0020172, and the Lawrence Livermore National Laboratory 'Microbes Persist' Soil Microbiome Scientific Focus Area (SCW1632) and by the National Science Foundation (No. DEB-1645596). Research conducted at Lawrence Livermore National Laboratory was supported by the Department of Energy Office of Science, via awards SCW1679 and SCW1590, conducted under the auspices of Department of Energy Contract DE-AC52- 07NA27344. Research conducted at Pacific Northwest National Laboratory was supported by the Department of Energy Office of Science, via awards FWP 68907 and FWP 74475, conducted under the auspices of Department of Energy Contract DE-AC05-76RL01830.

Data availability Sequence data and sample metadata have been previously deposited in NCBI Sequence Read Archive under the project number PRJNA521534. Any additional metadata and intermediate data products are available at https://github.com/bramstone/density-dependence-qSIP.

Code availability All analytical and statistical code has been made available at https://github.com/bramstone/density-dependence-qSIP.

Declarations

Conflict of interest The authors declare that they have no conflict of interest.

Ethics approval No ethical guidelines were required to conduct or publish this research.

Consent to participate No patient information was utilized during the course of this research.

Consent for publication No patient information was utilized during the course of this research.

References

Albright MBN, Gallegos-Graves LV, Feeser KL, Montoya K, Emerson JB, Shakya M, Dunbar J (2022) Experimental evidence for the impact of soil viruses on carbon cycling during surface plant litter decomposition. ISME Commun 2:1–8. https://doi.org/10.1038/s43705-022-00109-4

Aldén L, Demoling F, Bååth E (2001) Rapid method of determining factors limiting bacterial growth in soil. Appl Environ Microbiol 67:1830–1838. https://doi.org/10.1128/AEM.67.4.1830-1838.2001

Allee WC (1941) Integration of problems concerning protozoan populations with those of general biology. Am Nat 75:473–487

Ashelford KE, Day MJ, Fry JC (2003) Elevated abundance of bacteriophage infecting bacteria in soil. Appl Environ Microbiol 69:285–289. https://doi.org/10.1128/AEM.69.1.285

Bever JD, Platt TG, Morton ER (2012) Microbial population and community dynamics on plant roots and their feedbacks in plant communities. Annu Rev Microbiol 66:265–283. https://doi.org/10.1146/annurev-micro-092611-150107.Microbial

Blazewicz SJ, Hungate BA, Koch BJ, Nuccio EE, Morrissey E, Brodie EL et al (2020) Taxon-specific microbial growth and mortality patterns reveal distinct temporal population responses to rewetting in a California grassland soil. ISME J. https://doi.org/10.1038/s41396-020-0617-3

Bolyen E, Rideout JR, Dillon MR, Bokulich NA, Abnet CC, Al-Ghalith GA et al (2019) Reproducible, interactive, scalable and extensible microbiome data science using QIIME 2. Nat Biotechnol 37:852–857. https://doi.org/10.1038/s41587-019-0209-9

Braga LPP, Spor A, Kot W, Breuil MC, Hansen LH, Setubal JC et al (2020) Impact of phages on soil bacterial communities and nitrogen availability under different assembly scenarios. Microbiome 8:1–14. https://doi.org/10.1186/s40168-020-00822-z

Cabaço S, Apostolaki ET, García-Marín P, Gruber R, Hernández I, Martínez-Crego B et al (2013) Effects of nutrient enrichment on seagrass population dynamics: evidence and synthesis from the biomass-density relationships. J Ecol 101:1552–1562. https://doi.org/10.1111/1365-2745.12134

Cadotte MW, Mai DV, Jantz S, Collins MD, Keele M, Drake JA (2006) On testing the competition - colonization trade - off in a multispecies assemblage. Am Nat 168:704–709. https://doi.org/10.1086/508296

Callahan BJ, McMurdie PJ, Rosen MJ, Han AW, Johnson AJA, Holmes SP (2016) DADA2: high-resolution sample inference from Illumina amplicon data. Nat Methods 13:581–583. https://doi.org/10.1038/nmeth.3869

Campbell BD, Grime JP (1992) An experimental test of plant strategy theory. Ecology 73:15–29. https://doi.org/10.2307/1938717

Carson JK, Gonzalez-quin V, Murphy DV, Hinz C, Shaw JA, Gleeson DB (2010) Low pore connectivity increases bacterial diversity in soil. Appl Environ Microbiol 76:3936–3942. https://doi.org/10.1128/AEM.03085-09

Chesson P (2000) Mechanisms of maintenance of species diversity. Annu Rev Ecol Syst 31:343–358

Connell JH (1971) On the role of natural enemies in preventing competitive exclusion in some marine animals and in rain forest trees. In: den Boer PJ, Gradwell GR (eds) Dynamics of Populations. Center for Agricultural Publishing and Documentation, Wageningen, The Netherlands, pp 298–312

Dang C, Walkup JGV, Hungate BA, Franklin RB, Schwartz E, Morrissey EM (2021) Phylogenetic organization in the assimilation of chemically distinct substrates by soil bacteria. Environ Microbiol. https://doi.org/10.1111/1462-2920.15843

de Vries FT, Griffiths RI, Bailey M, Craig H, Girlanda M, Gweon HS et al (2018) Soil bacterial networks are less stable under drought than fungal networks. Nat Commun. https://doi.org/10.1038/s41467-018-05516-7

Delgado-Baquerizo M, Reich PB, Khachane AN, Campbell CD, Thomas N, Freitag TE et al (2017) It is elemental: soil nutrient stoichiometry drives bacterial diversity. Environ Microbiol 19:1176–1188. https://doi.org/10.1111/1462-2920.13642

Demoling F, Figueroa D, Bååth E (2007) Comparison of factors limiting bacterial growth in different soils. Soil Biol Biochem 39:2485–2495. https://doi.org/10.1016/j.soilbio.2007.05.002

Erez Z, Steinberger-levy I, Shamir M, Doron S, Stokar-Avihail A, Peleg Y et al (2017) Communication between viruses guides lysis – lysogeny decisions. Nature 541:488–493. https://doi.org/10.1038/nature21049

Fierer N, Jackson RB (2006) The diversity and biogeography of soil bacterial communities. Proc Natl Acad Sci U S A 103:626–631. https://doi.org/10.1073/pnas.0507535103

Flemming H-C, Wuertz S (2019) Bacteria and archaea on Earth and their abundance in biofilms. Nat Rev Microbiol 17:247–260. https://doi.org/10.1038/s41579-019-0158-9

Gause GF (1934) The Struggle for Existence. Williams and Wilkins Company, Baltimore, MD

Hibbing ME, Fuqua C, Parsek MR, Peterson SB (2010) Bacterial competition: surviving and thriving in the microbial jungle. Nat Rev Microbiol 8:15–25. https://doi.org/10.1038/nrmicro2259

Howard-Varona C, Hargreaves KR, Abedon ST, Sullivan MB (2017) Lysogeny in nature: mechanisms, impact and ecology of temperate phages. ISME J 11:1511–1520. https://doi.org/10.1038/ismej.2017.16

Hungate BA, Mau RL, Schwartz E, Caporaso JG, Dijkstra P, van Gestal N et al (2015) Quantitative microbial ecology through stable isotope probing. Appl Environ Microbiol 81:7570–7581. https://doi.org/10.1128/AEM.02280-15

Janzen DH (1970) Herbivores and the number of tree species in tropical forests. Am Nat 104:501–528. https://doi.org/10.1086/282687

Jessup CM, Forde SE, Bohannan BJM (2005) Microbial experimental systems in ecology. Adv Ecol Res 37:273–307. https://doi.org/10.1016/S0065-2504(04)37009-1

Johnson DJ, Beaulieu WT, Bever JD, Clay K (2012) Conspecific negative density dependence and forest diversity. Science 336:904–907. https://doi.org/10.1126/science.1220269

Jukes TH, Cantor CR (1969) Evolution of protein molecules. In: Munro H (ed) Mammalian Protein Metabolism, vol 3. Academic Press. New York, NY, pp 21–132

Kaul RB, Kramer AM, Dobbs FC, Drake JM (2016) Experimental demonstration of an Allee effect in microbial populations. Biol Lett. https://doi.org/10.1098/rsbl.2016.0070

Kerr B, Riley MA, Feldman MW, Bohannan BJM (2002) Local dispersal promotes biodiversity in a real-life game of rock-paper-scissors. Nature 418:171–174. https://doi.org/10.1038/nature00823

Klironomos JN (2002) Feedback with soil biota contributes to plants rarity and invasiveness in communities. Nature 417:67–69. https://doi.org/10.1038/417067a

Koch BJ, McHugh TA, Hayer M, Schwartz E, Blazewicz SJ, Dijkstra P et al (2018) Estimating taxon-specific population dynamics in diverse microbial communities. Ecosphere. https://doi.org/10.1002/ecs2.2090

Kuzyakov Y, Mason-Jones K (2018) Viruses in soil : nano-scale undead drivers of microbial life, biogeochemical turnover and

ecosystem functions. Soil Biol Biochem 127:305–317. https://doi.org/10.1016/j.soilbio.2018.09.032
Letten AD, Dhami MK, Ke PJ, Fukami T (2018) Species coexistence through simultaneous fluctuation-dependent mechanisms. Proc Natl Acad Sci U S A 115:6745–6750. https://doi.org/10.1073/pnas.1801846115
Levine JM, HilleRisLambers J (2009) The importance of niches for the maintenance of species diversity. Nature 461:254–257. https://doi.org/10.1038/nature08251
Li J, Mau RL, Dijkstra P, Koch BJ, Schwartz E, Liu XJA et al (2019) Predictive genomic traits for bacterial growth in culture versus actual growth in soil. ISME J 13:2162–2172. https://doi.org/10.1038/s41396-019-0422-z
Liu XJA, Sun J, Mau RL, Finley BK, Compson ZG, van Gestel N et al (2017) Labile carbon input determines the direction and magnitude of the priming effect. Appl Soil Ecol 109:7–13. https://doi.org/10.1016/j.apsoil.2016.10.002
Liu XJA, Finley BK, Mau RL, Schwartz E, Dijkstra P, Bowker MA et al (2020) The soil priming effect: consistent across ecosystems, elusive mechanisms. Soil Biol Biochem 140:107617. https://doi.org/10.1016/j.soilbio.2019.107617
Louca S, Doebeli M, Parfrey LW (2018) Correcting for 16S rRNA gene copy numbers in microbiome surveys remains an unsolved problem. Microbiome 6:1–12. https://doi.org/10.1186/s40168-018-0420-9
Maslov S, Sneppen K (2017) Population cycles and species diversity in dynamic Kill-the-Winner model of microbial ecosystems. Sci Rep 7:1–8. https://doi.org/10.1038/srep39642
Morris EC (2003) How does fertility of the substrate affect intraspecific competition? Evidence and synthesis from self-thinning. Ecol Res 18:287–305. https://doi.org/10.1046/j.1440-1703.2003.00555.x
Morrissey EM, Mau RL, Schwartz E, Caporaso JG, Dijkstra P, van Gestel N et al (2016) Phylogenetic organization of bacterial activity. ISME J 10:2336–2340. https://doi.org/10.1038/ismej.2016.28
Morrissey EM, Mau RL, Schwartz E, McHugh TA, Dijkstra P, Koch BJ et al (2017) Bacterial carbon use plasticity, phylogenetic diversity and the priming of soil organic matter. ISME J 11:1890–1899. https://doi.org/10.1038/ismej.2017.43
Morrissey EM, Mau RL, Hayer M, Liu XJA, Schwartz E, Dijkstra P et al (2019) Evolutionary history constrains microbial traits across environmental variation. Nat Ecol Evol. https://doi.org/10.1038/s41559-019-0918-y
Nadell CD, Drescher K, Foster KR (2016) Spatial structure, cooperation and competition in biofilms. Nat Rev Microbiol 14:589–600. https://doi.org/10.1038/nrmicro.2016.84
Nakagawa S, Johnson PCD, Schielzeth H (2017) The coefficient of determination R2 and intra-class correlation coefficient from generalized linear mixed-effects models revisited and expanded. J R Soc Interface. https://doi.org/10.1098/rsif.2017.0213
Pedregosa F, Varoquaux G, Gramfort A, Michel V, Thirion B, Grisel O et al (2011) Scikit-learn: Machine Learning in Python. J Mach Learn Res 12:2825–2830. https://doi.org/10.1007/s13398-014-0173-7.2
Petermann JS, Fergus AJF, Turnbull LA, Schmid B (2008) Janzen-Connell effects are widespread and strong enough to maintain diversity in grasslands. Ecology 89:2399–2406. https://doi.org/10.1890/07-2056.1
Phaiboun A, Zhang Y, Park B, Kim M (2015) Survival kinetics of starving bacteria is biphasic and density-dependent. PLoS Comput Biol 11:1–18. https://doi.org/10.1371/journal.pcbi.1004198
Quast C, Pruesse E, Yilmaz P et al (2013) The SILVA ribosomal RNA gene database project: Improved data processing and web-based tools. Nucleic Acids Res 41:590–596. https://doi.org/10.1093/nar/gks1219
Raynaud X, Nunan N (2014) Spatial ecology of bacteria at the microscale in soil. PLoS ONE. https://doi.org/10.1371/journal.pone.0087217
Rovere J, Fox JW (2019) Persistently rare species experience stronger negative frequency dependence than common species: a statistical attractor that is hard to avoid. Glob Ecol Biogeogr 28:508–520. https://doi.org/10.1111/geb.12871
Steen H, Scrosati R (2004) Intraspecific competition in Fucus serratus and F. evanescens (Phaeophyceae: Fucales) germlings: effects of settlement density, nutrient concentration, and temperature. Mar Biol 144:61–70. https://doi.org/10.1007/s00227-003-1175-8
Stoddard SF, Smith BJ, Hein R, Roller BRK, Schmidt TM (2015) rrnDB: improved tools for interpreting rRNA gene abundance in bacteria and archaea and a new foundation for future development. Nucleic Acids Res 43:D593–D598. https://doi.org/10.1093/nar/gku1201
Stone BW, Li J, Koch BJ, Blazewicz SJ, Dijkstra P, Hayer M et al (2021) Nutrients cause consolidation of soil carbon flux to small proportion of bacterial community. Nat Commun 12:1–9. https://doi.org/10.1038/s41467-021-23676-x
Tecon R, Or D (2017) Biophysical processes supporting the diversity of microbial life in soil. FEMS Microbiol Rev. https://doi.org/10.1093/femsre/fux039
Tilman D (1977) Resource competition between plankton algae: an experimental and theoretical approach. Ecology 58:338–348
Trubl G, Bin JH, Roux S, Emerson JB, Solonenko N, Vik DR et al (2018) Soil viruses are underexplored players in ecosystem carbon processing. Msystems 3:1–21. https://doi.org/10.1128/msystems.00076-18
Vidakovic L, Singh PK, Hartmann R, Nadell CD, Drescher K (2018) Dynamic biofilm architecture confers individual and collective mechanisms of viral protection. Nat Microbiol 3:26–31. https://doi.org/10.1038/s41564-017-0050-1
Wang A, Jiang XX, Zhang QQ, Zhou J, Li HL, Luo FL et al (2015) Nitrogen addition increases intraspecific competition in the invasive wetland plant *Alternanthera philoxeroides*, but not in its native congener *Alternanthera sessilis*. Plant Spec Biol 30:176–183. https://doi.org/10.1111/1442-1984.12048
Williamson KE, Fuhrmann JJ, Wommack KE, Radosevich M (2017) Viruses in soil ecosystems : an unknown quantity within an unexplored territory. Annu Rev Virol. https://doi.org/10.1146/annurev-virology-101416-041639
Wright ES (2016) Using DECIPHER v2.0 to analyze big biological sequence data in R. R J 8:325–359
Young IM, Crawford JW, Nunan N, Otten W (2008) Microbial Distribution in Soils : Physics and Scaling. In: Advances in Agronomy, 1st edn. Elsevier Inc., pp 81–121